worldwide UHF RFID frequency band. The measured maximum reading distance of a single tag is 5 m, and the concurrent reading distance of 19 arranged tags using a single reader is 1 m in the x-axis direction. As the proposed tag antenna has broadband characteristics and concurrent reading capability, it is a good candidate for UHF RFID library management systems.

ACKNOWLEDGMENTS

This work was supported by the Seoul R&BD Program (10848), Korea.

REFERENCES

1. K. Finkenzeller, RFID Handbook, Carl Hanser Verlag GmbH & Co. KG, 2002.
2. C.A. Balanis, Antenna Theory, Analysis and Design, 2nd ed., Wiley, New York, 1997.
3. H.W. Son and C.S. Tyo, Design of RFID tag antennas using an inductively coupled feed, Electron Lett 41 (2005), 994–996.
4. G. Marrocco, Body-matched antenna for wireless biometry, In: European Conference on Antennas and Propagation, Nice, France, 2006, p 795.
5. K. Kurokawa, Power waves and the scattering matrix, IEEE Trans Microwave Theory Tech 13 (1964), 194–202.
6. P.V. Nikitin, K.V. Seshagiri Rao, S.F. Lam, V. Pillai, R. Martinez, and H. Heinrich, Power reflection coefficient analysis for complex impedances in RFID .pb2 Tag design, IEEE Trans Microwave Theory Tech 53 (2005), 2721–2725.
7. W.L. Stutzman, and G.A. Thiele, Antenna Theory and Design, 2nd ed., Wiley, New York, 1998, Ch. 5.
8. K.H. Awadalla, A.-E.-M. Sharshar, A simple method to determine the impedance of a loop antenna, IEEE Trans Antennas Propag AP-32 (1984), 1248–1251.
9. H.M. Greenhouse, Design of planar rectangular microelectronic inductors, IEEE Trans Parts Hybrid Packag 10 (1974), 101–109.
10. F.W. Grover, Inductance Calculations, Van Nostrand, Princeton, NJ, 1946; reprinted by Dover Publications, New York, 1962.
11. C.S. Walker, Capacitance, Inductance, and Crosstalk analysis, Artech House, Denham, 1990.
12. http://www.impinj.com

DESIGN OF VERTICAL LINES FOR VEHICLE REAR WINDOW ANTENNAS

Woojoon Kang and Hosung Choo
School of Electronic and Electrical Engineering, Hongik University, Seoul, Korea; Corresponding author: hschoo@hongik.ac.kr

Received 6 September 2009

ABSTRACT: *In this article, we propose the design of a rear on-glass antenna for a commercial sedan. We focus on optimizing the vertical lines of the antenna and propose the optimum design parameters to maximize the matching bandwidth and improve the average vertical gain for the entire FM radio band. The detailed design parameters are determined using the Pareto genetic algorithm with an EM simulation tool. The optimized rear on-glass antenna was built and installed on a commercial sedan. The measurement results showed a matching bandwidth of about 15%, an average bore-sight gain of about −2.86 dBi in the entire FM band, and an average gain of about −14 dBi along the azimuth direction.* © 2010 Wiley Periodicals, Inc. Microwave Opt Technol Lett 52: 1445–1449, 2010; Published online in Wiley InterScience (www.interscience.wiley.com). DOI 10.1002/mop.25184

Key words: *vehicle antenna; rear on-glass antenna; vertical lines*

1. INTRODUCTION

An FM radio receiver is by far the most common device in commercial vehicle, and its performance of good signal reception is dominantly determined by an antenna, which is generally a monopole that protrudes outside the vehicle [1]. Recently, to improve the durability and appearance and to reduce the wind noise of a pole-type FM antenna, an internal on-glass antenna that is directly printed on a rear or a quarter window has been widely adopted by newer sedan models [2–4]. The internal on-glass antenna, however, often exhibits low-radiation gain and narrow matching bandwidth characteristics because the antenna is printed on the lossy dielectric material of the window glass and the conductivity of the stripline is restricted due to its dual function as defroster lines.

To improve antenna performance, the rear window antenna usually has multiple vertical lines between horizontal defroster lines. By loading these vertical lines, the current distributions are altered so as to increase the vertical antenna gain and to improve the impedance matching with the FM radio tuner. Although loading the vertical lines is the key technology in determining the performance of on-glass antennas, in-depth research on this topic has not been undertaken to date.

In this article, we report on the design of the rear window antenna. We focus our research primarily on optimizing vertical lines, and we propose the optimum design parameters, such as number, length, position, and angle of vertical lines. Some design limitations exist due to the aesthetic design requirements for vehicles, such as vertical lines should be placed symmetrically and cannot exceed a certain number. We obtain optimum parameters under these design restrictions, using a Pareto genetic algorithm (PGA) in conjunction with a full-wave EM simulator. In the optimization process, two objective functions are used to maximize the matching bandwidth in the FM band and to increase the average vertical antenna gain. To verify the optimized result, the optimum design is printed on a rear window of a commercial vehicle and its antenna performances, such as bandwidth, radiation pattern, and antenna gain, are measured. The results show that the average vertical gain and the matching bandwidth improve as the number of vertical lines increases. These results confirm that the proposed design is applicable for a rear on-glass antenna on a commercial vehicle.

2. ANTENNA STRUCTURE AND OPTMIZATION

Figure 1 shows the geometry of the proposed rear on-glass antenna, which consists of 15 horizontal defroster lines and multiple vertical lines. Design parameters of the vertical lines are given by the number (N), the length (L_1, L_2, and L_3), the distance from the center of the horizontal defroster lines (W_1, W_2,

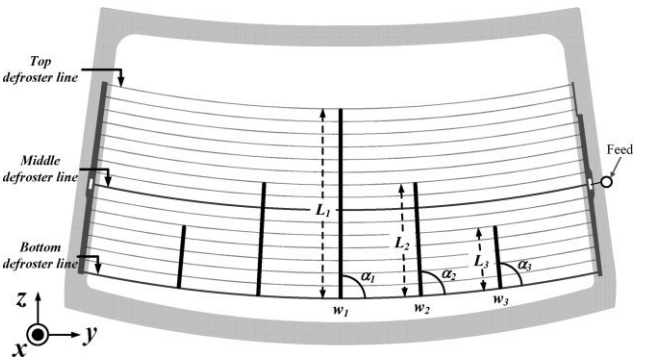

Figure 1 Geometry of the rear on-glass antenna

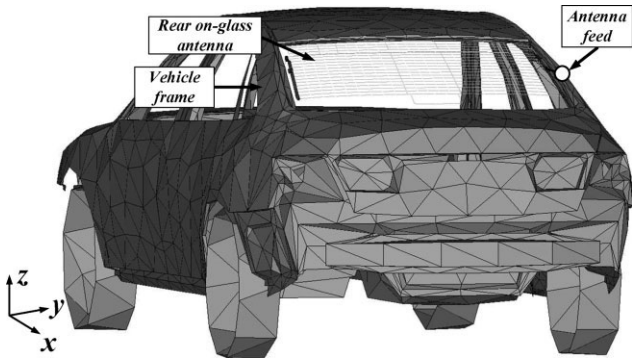

Figure 2 The vehicle model for the on-glass antenna

and W_3), and the angle (θ_1 and θ_2) in which horizontal and vertical lines intersect. Because of exterior design restrictions, the maximum number of vertical lines is limited to five and the vertical lines are left–right symmetric with respect to the center of the horizontal defroster lines. To accurately estimate the rear on-glass antenna's performance, we used a FEKO of EM Software and Systems [5]. In our EM simulation, we used the equivalent coated wire method to improve the accuracy and the simulation speed. The equivalent conditions for the coated wire are given by 0.1-mm diameter for the conducting core ($\sigma = 5.7 \times 10^7$ S/m) and 12-mm diameter for the dielectric coating ($\varepsilon_r = 8$, $\tan\delta = 0.03$ at 100 MHz) [6–8].

Because the size of the vehicle body is in the order of wavelength in the FM band, the input impedance and the radiation pattern are significantly changed by the specific geometry of the vehicle, such as the position of the window, the feed position, and the shape of the vehicle frame. It is impossible to estimate accurate results if the vehicle structure is omitted from the EM simulation, and thus we included the whole vehicle body as triangular piecewise meshes. The meshes of the vehicle model used in our EM simulation are shown in Figure 2. Although the simulation accuracy is improved further with a denser mesh model, we set the mesh number to be below 4000, which allows for 2 min in the EM simulation per each frequency and maintains an accuracy rate of greater than 80% compared with the measurement as shown in Figure 3.

To obtain the detailed design parameters (L_1, L_2, L_3, W_1, W_2, α_1, and α_2) and achieve the stated design goals of broad bandwidth and high-vertical gain, we used the PGA [9] in conjunction with the FEKO EM simulation tool [5]. The cost functions

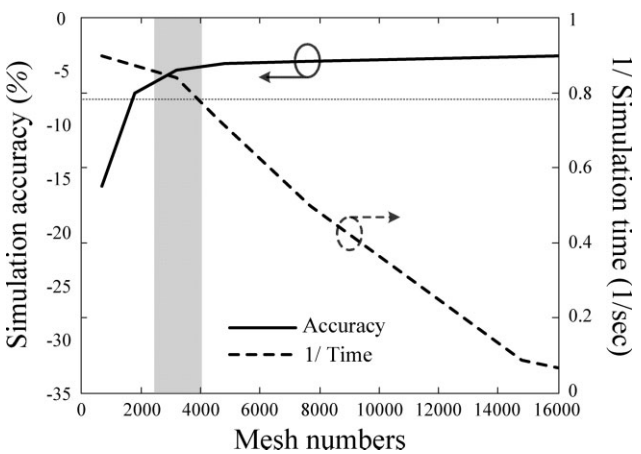

Figure 3 Accuracy and simulation time vs. mesh numbers

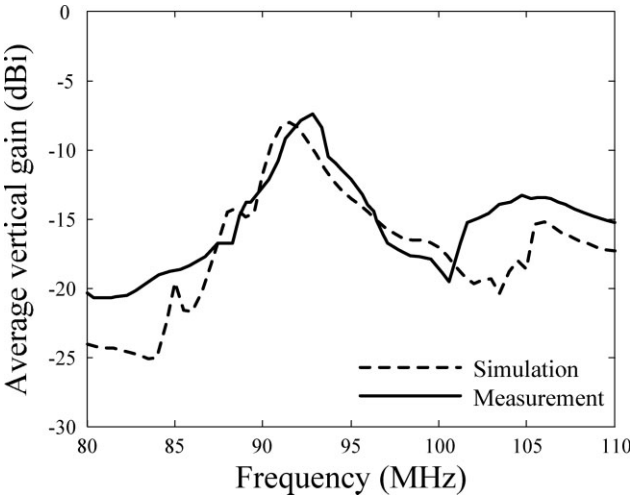

Figure 4 Average vertical gain of the optimized antenna

of the PGA to produce the optimized design parameters are given in (1) and (2).

$$Cost1 = 1 - \frac{BW_{\mathrm{Ant}}}{BW_{\mathrm{FM}}}, \tag{1}$$

$$Cost2 = \frac{1}{MN}\sum_{i=1}^{M}\sum_{j=1}^{N}\{Gain(f_i, \theta = 90^{\circ}, \phi_j)\}, \tag{2}$$

$$0^{\circ} < \phi_j \le 360^{\circ}, 80\mathrm{MHz} \le f_i \le 110\mathrm{MHz}.$$

Equation (1) is used to broaden bandwidth in the FM radio band. BW_{FM} means the bandwidth of the entire FM band (30 MHz, 80 $\sim$ 110 MHz), and BW_{Ant} is the half power bandwidth (VSWR <5.8) of the antenna. To maintain omni-directional radiation pattern, which is an important characteristic of the vehicle antenna, Eq. (2) is adopted to reduce the variation of the average vertical gain in the azimuth direction.

3. SIMULATION AND MEASUREMENT RESULTS

To examine the effect of the vertical lines on antenna performance, we first used only three variables of vertical lines,

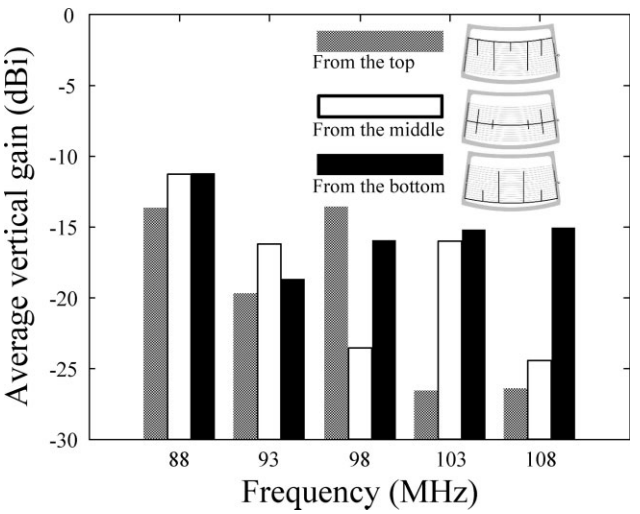

Figure 5 Average vertical gain vs. each starting point

including the number (N), the length (L_1, L_2,…), and the distance (W_1, W_2,…), while the angle variable was fixed as 90°. We then obtained the optimized design based on the EM simulation and PGA optimization described in Section 2. To verify the optimized results, we built and installed the antenna on the rear window of 2009 TG Grandeur, which is a commercial sedan from Hyundai Motors company [10]. We used an Agilent E5071A network analyzer with an ETS-Lindgren 3121C dipole [11] as the transmitter antenna and measured the optimized design in a semi-anechoic chamber having dimensions of 30 m × 30 m. In Figure 4, the simulated and measured results of average vertical gain are plotted as a dashed and solid line, respectively, and they show good agreement.

To explore the antenna performance against the starting point of the vertical line, we compared the antenna performance to each optimized design where the vertical lines start from the top, the middle, and the bottom defroster lines. The resulting average vertical gain in the azimuth direction is illustrated in Figure 5, and the design with the vertical lines starting from the bottom exhibits the best performance of more than −18 dBi in comparison with other cases.

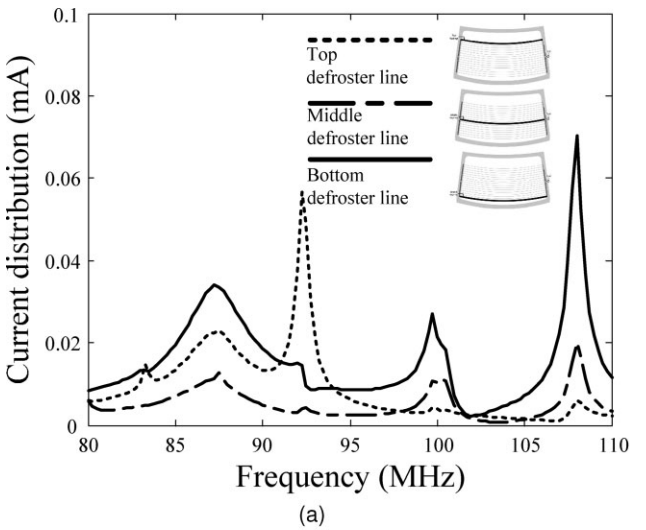

Figure 6 Space-averaged current distribution. (a) Defroster line current distribution and (b) vertical line current distribution

TABLE 1 Design Parameters for the Rear On-Glass Antennas

Ant. 1 ($N = 5$, mm)					
L_1	240	W_1	0	α_1	90°
L_2	360	W_2	150	α_2	96°
L_3	210	W_3	390	α_3	100°
Ant. 2 ($N = 2$, mm)					
L_2	450	w_2	120	α_2	93°

To understand the reason that performance varies with respect to the starting point, we examined the current distribution on each horizontal defroster line and vertical line. In Figure 6(a), we simulated space-averaged current distribution only on each horizontal defroster line excluding the effects of vertical lines. The simulation showed that the most current is induced on the bottom horizontal defroster line at the operating frequency. As a result, vertical lines starting from the bottom defroster line are shown to have more induced currents than other cases, as illustrated in Figure 6(b).

To increase design freedom of the vertical lines, we added the angle variable, which is where horizontal and vertical lines intersect. We then found the optimum design parameters using PGA with EM simulation. The final design parameters of the optimized antenna (Ant. 1) are listed in Table 1. In the same table, we include the design parameters of a commercial on-glass antenna (Ant. 2) using only two vertical lines for comparison with our optimized design. The measured bore-sight gain of the Ant. 1 and the Ant. 2 are shown in Figure 7. The Ant. 1 shows a bore-sight gain of more than −12 dBi in the entire FM radio band (from 80 to 110 MHz), with an average gain of −2.86 dBi, which is superior to that of the Ant. 2 by more than 7.2 dB on average.

To examine the omni-directional properties, we also measured the radiation pattern of antennas in the whole azimuth direction. As shown in Figure 8, the maximum radiation gain of Ant. 1 occurs in the bore-sight direction ($\theta = 90°$, $\phi = 0°$), and the average vertical gain in the entire azimuth direction exceeds −14 dBi at 88 MHz, 98 MHz, and 108 MHz. The Ant. 1 shows better performance than the Ant. 2 at an average of 5 dB. To verify antenna performance under a real outdoor condition, we conducted field tests to measure the received signal power of

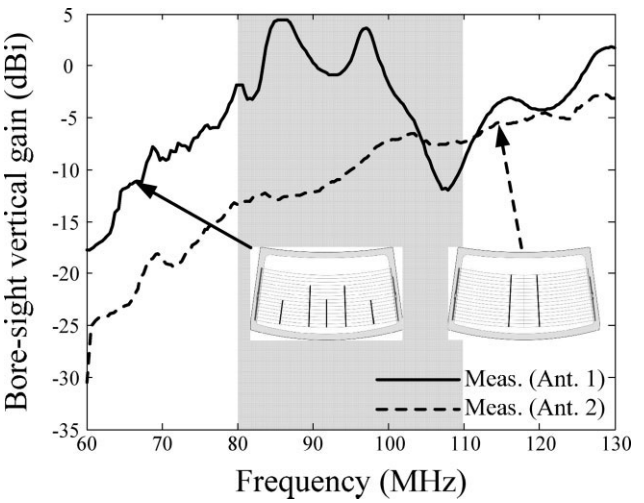

Figure 7 Optimized design vs. commercial design

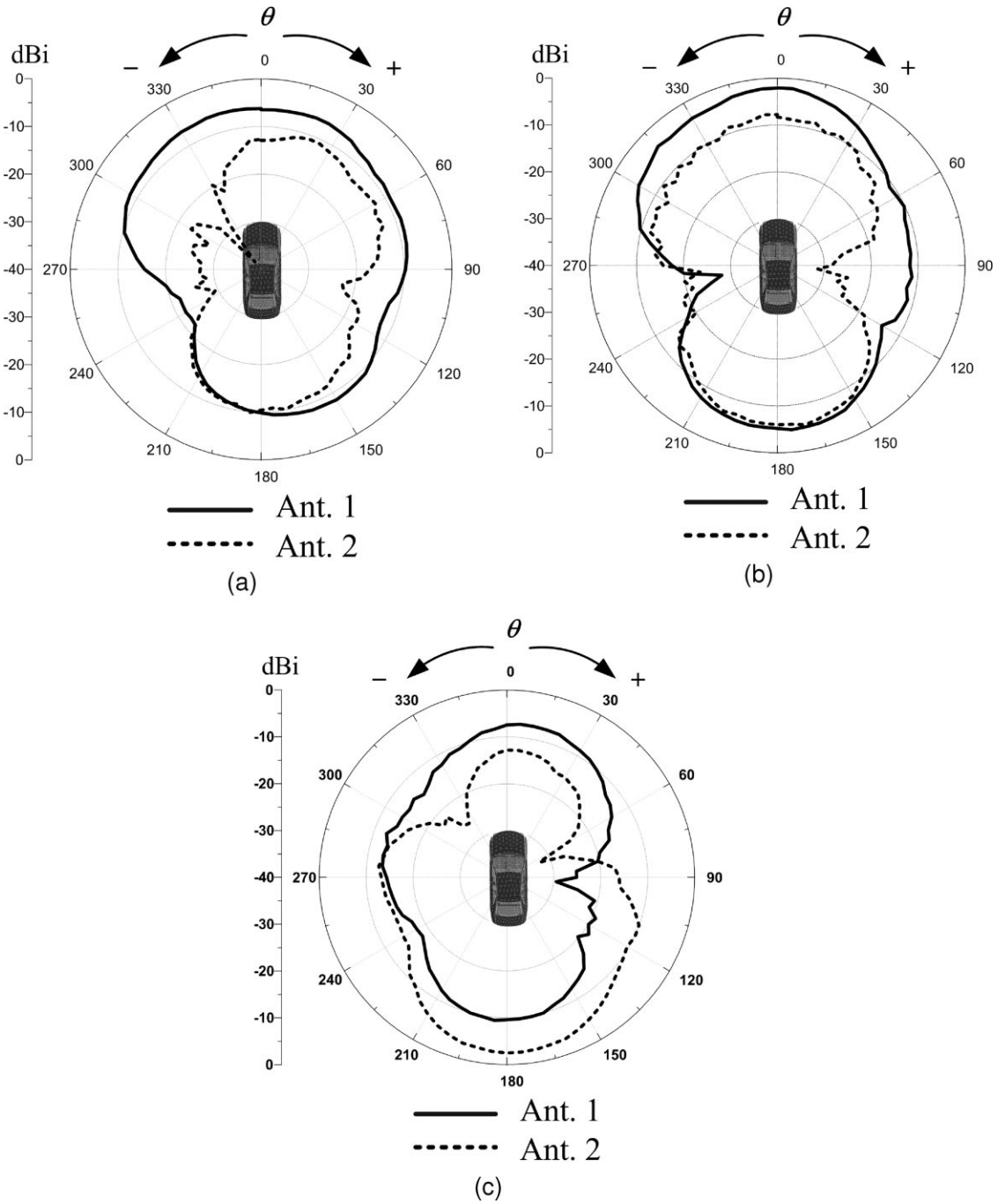

Figure 8 Radiation patterns in the azimuth direction. (a) 88 MHz, (b) 98 MHz, and (c) 108 MHz

each antenna from the base station. The measurement site selected was in Mapo-gu, Seoul, Korea, and the driving speed of the vehicle was about 60 km h^{-1}. To accurately measure the received signal power, we used a spectrum analyzer connected to the feed of the rear on-glass antenna and collected the power level in real time at a sampling rate of 3 Hz (8 min per each site). The performance of the Ant. 1, on average, 11 dB better than that of the Ant. 2 (Table 2).

4. CONCLUSIONS

In this article, we reported on the design of the rear on-glass antenna for a commercial vehicle. We set four variables of

TABLE 2 Received Signal Power of Each Antenna under Real Outdoor Conditions

Received power (dBm)	Site 1	Site 2	Site 3	Site 4	Site 5	Avg.
Ant. 1	−46	−38	−35	−40	−50	−42.15
Ant. 2	−57	−48	−45	−50	−63	−53.46

vertical lines, including the number, distance, length, and angle. To obtain optimum parameters, we used a PGA in conjunction with a full-wave EM simulation tool to maximize the matching bandwidth and to increase the average vertical gain in the FM band. To verify our PGA results, we built and installed the optimized antenna on a conventional vehicle, and the antenna performances were measured in a semi-anechoic chamber. The measurement results of the optimized rear on-glass antenna showed a matching bandwidth (VSWR <5.8) of about 15% in the FM radio band, a vertical gain of about -2.86 dBi along the bore-sight direction, and an average gain of about -14 dBi along the azimuth direction.

ACKNOWLEDGMENTS

This research was supported by Hyundai·Kia Motors and the IT R&D program of MKE/IITA in Korea (2009-F-042-01, A Study on Mobile Communication System for Next-Generation Vehicles with Internal Antenna Array).

REFERENCES

1. D. Bolle and M. Morganstern, Monopole and conic antennas on spherical vehicle, IEEE Trans Antennas Propag 17 (1969), 477–484.
2. R. Abou-Jaoude and E.K. Walton, Numerical modeling of on-glass conformal automobile antennas, IEEE Trans Antennas Propag 46 (1998), 845–852.
3. Y. Noh, Y. Kim, and H. Ling, Broadband on-glass antenna with mesh-grid structure for automobiles, Electron Lett 41 (2005), 1148–1149.
4. J.C. Batchelor, R.J. Langley, and H. Endo, On-glass mobile antenna performance modeling, IEE Proc Microwave Antennas Propag 148 (2001), 233–238.
5. FEKO Suite 5.3, EM Software and Systems, 2007. Available at http://www.feko.info.
6. J. Moore, Simplified analysis of coated wire antennas and scatterers, IEE Proc Microwave Antennas Propag 142 (1995), 14–18.
7. A. Chatterjee, J.L. Volakis, and W.J. Kent, Scattering by a perfectly conducting and coated thin wires using a physical basis model, IEEE Trans Antennas Propag 40 (1992), 761–769.
8. U. Pekel, N. Wang, and L. Peters, An equivalent model for the analysis of electromagnetic scattering from a long, lossy tether structure, IEEE Trans Antennas Propag 40 (1992), 1555–1561.
9. Y. Rahmat-Samii and E. Michielssen, Electromagnetic optimization by genetic algorithms, Wiley, New York, 1999.
10. TG grandeur, 2009. Available at http://www.hyundai.com.
11. Transmit antenna. Available at http://www.ets-indgren.com/manuals/3121C.pdf.

EVALUATION OF EMI RISK DUE TO THE INTERACTION BETWEEN CELLULAR PHONES AND MEDICAL DEVICES

Hsing-Yi Chen and Cheng-Yi Chou

Department of Communications Engineering, Yuan Ze University, 135, Yuan-Tung Road, Nei-Li, Chung-Li, Taoyuan Shian, Taiwan 320, Republic of China; Corresponding author: eehychen@saturn.yzu.edu.tw

Received 8 September 2009

ABSTRACT: *The FDTD method was used to calculate the electric fields emitted from cellular phones. Cellular phones were modeled by a quarter-wavelength monopole antenna mounted on a rectangular box with equivalent material in the interior of the rectangular box and a dielectric coating in the exterior of the rectangular box. Measurements of the electric fields emitted from cellular phones were also performed by using a Narda Model SRM-3000 high frequency selective radiation meter with an isotropic* E*-field probe. From measurement and simulation results, electric fields emitted from cellular phones are in the range of 0.02–39.0 V/m for separation distances of 0–3 m between handsets and test points. It is found that field strengths emitted from cellular phones may meet the recommended EMI immunity level of 3 V/m set by the IEC for medical equipment keeping a separation distance of more than 1 m from cellular phones. An interference threshold separation distance of 3 m is proposed for evaluating the interaction between cellular phones and medical devices.* © 2010 Wiley Periodicals, Inc. Microwave Opt Technol Lett 52: 1449–1454, 2010; Published online in Wiley InterScience (www.interscience.wiley.com). DOI 10.1002/mop.25221

Key words: *FDTD; cellular phone; field strength; interference*

1. INTRODUCTION

As digital cellular phones become widely used, the electromagnetic interference (EMI) on medical environment becomes a growing concern among hospital and clinic staffs, electronics manufacturers, and government regulatory agencies. Because the effects of EMI on medical devices may affect a patient's life, the interaction between cellular phones and medical devices such as apnea monitors, implanted defibrillators, implanted heart pacemakers, operating machines, powered wheelchairs, and hearing aids should be well studied. Digital cellular phones may emit higher strength peak electromagnetic fields than do analogy cellular phones. Because they work with digital bit streams, which can be thought as strings of ones and zeros, digital cellular phones may induce spurious currents or voltages in medical devices, and thus introduce an EMI problem to the medical equipment. It is extremely difficult and costly to study these EMI problems. Many factors need to be taken into account when studying this problem, including the type of emitting device, the emitting power of a cellular phone, frequency and modulation scheme of a cellular phone, locations of medical instruments, relative orientation between cellular phones and medical instruments, and the technology used by a cellular phone. Cellular phones may be used in different modes such as standby, full-power transmission, communication (ringing and talkback), and initiation. Each mode has a different emitting power level and working time. Cellular phones also have power control features that seek to minimize output power when transmitting information. Certain medical equipment may be more susceptible to interference from specific frequencies. A confluence of several cellular phones operating on similar EM frequencies may also enhance the potential for EMI. Because of the absorption and reflection of EM waves by the physical environment, the medical devices situated in a hospital may also affect the chances of EMI occurring. Emission field strengths from cellular phones can occasionally be higher than expected at greater distances and lower than expected at lesser distances. Some experimental studies on the interference between cellular phones and medical devices have been reported in the literature [1–7]. However, only a few theoretical studies on the evaluation of EMI due to the interaction between cellular phones and medical devices are reported [8, 9]. In this article, the finite-difference time-domain (FDTD) method [10] was used to calculate the electric fields emitted from cellular phones. Cellular phones were modeled by a quarter-wavelength monopole antenna mounted on a rectangular box with equivalent material in the interior of the rectangular box and a dielectric coating in the